Ring-eye blue beads in Iron Age central Italy – Preliminary discussion of technology and possible trade connections

RING-EYE BLUE BEADS IN IRON AGE CENTRAL ITALY – PRELIMINARY DISCUSSION OF TECHNOLOGY AND POSSIBLE TRADE CONNECTIONS

Oleh Yatsuk[(1,*)], Astrik Gorghinian[(2)], Giacomo Fiocco[(3,4)], Patrizia Davit[(1)], Serena Francone[(5)], Alessandra Serges[(5)], Leonie Koch[(6)], Alessandro Re[(7)], Alessandro Lo Giudice[(7)], Marco Ferretti[(8)], Marco Malagodi[(3,4)], Cristiano Iaia[(9)] and Monica Gulmini[(1)]

(1) Department of Chemistry, University of Turin, Via Giuria 7, 10125 Torino (Italy).
(2) National Institute of Nuclear Physics, National Laboratory of Frascati, via Enrico Fermi 40, 00044, Frascati, Roma (Italy).
(3) Arvedi Laboratory of Non-Invasive Diagnostics, CISRiC, University of Pavia, Via Bell'Aspa 3, 26100 Cremona (Italy).
(4) Department of Musicology and Cultural Heritage, University of Pavia, Corso Garibaldi 178, 26100 Cremona (Italy).
(5) Museo delle Civiltà, piazza Guglielmo Marconi 14, 00144 Rome (Italy).
(6) Institute of Prehistory and Early History, University of Cologne, Weyertal 125, 50931 Köln (Germany).
(7) Department of Physics, University of Turin and INFN Turin Division, Via Pietro Giuria 1, 10125 Torino (Italy).
(8) Italian National Research Council, Institute of Heritage Sciences, A.d.R. RM1, Via Salaria km 29.300, 00015 Montelibretti, Roma (Italy).
(9) Department of Historical studies, University of Turin, Via Sant'Ottavio 20, 10124 Torino (Italy).

*Corresponding author, oleh.yatsuk@unito.it

ABSTRACT. The Iron Age was a remarkable period in glass technology development and its spread across the Mediterranean. Communities that populated what is nowadays Central Italy underwent profound changes during this period forming more complex societies, developing proto-urban and urban centres, and incorporating into a wide trade network of the Mediterranean Sea and beyond. Glass objects in that small region are frequently found in burial sites dated to the first half of the first millennium BCE, with small blue beads with simple ring eyes being among the most abundant types. Fifty-six objects of this type (both whole beads and fragments) were studied with a non-invasive approach by means of Optical Microscopy, Fibre Optics Reflectance Spectroscopy, and portable X-Ray Fluorescence spectroscopy. The analyses were conducted *in situ* at the Museo Nazionale Etrusco di Villa Giulia and at the Museo delle Civiltà (both in Rome, Italy). Five samples from the main set were also analysed with a Scanning Electron Microscope coupled to an Energy Dispersive Spectrometer. The data gave preliminary information on the raw materials used to prepare the glass, the manufacturing techniques, and offered some hints to (tentatively) locate the region of provenance. In particular, the analyses established that the beads are soda-lime-silica glass and the source of cobalt, used as the blue colorant, could be an ore from Egypt. Within this general frame, a smaller group showed a different compositional pattern. These preliminary results contribute new knowledge for tracing exchange routes within the Mediterranean during the Iron Age.

KEYWORDS: glass, Iron Age, beads, FORS, p-XRF.

1. INRODUCTION.

This study is the first systematic investigation - performed mainly through a non-invasive approach - of ring-eye blue beads, which are among the earliest glass bead types from the Early Iron Age (EIA) contexts in the Italian peninsula. Because such beads are frequently found, the archaeological inferences can take great advantage from the determination of the chemical composition of the glass. Compositional homogeneity - or heterogeneity - within a set of beads can, in fact, give clues to define at least the number of glass-making sites

that were covering the demand of such items. Moreover, in some instances, compositional features may give useful information to locate the production sites (Shortland et al. 2007; Conte et al. 2016; Oikonomou et al. 2018; Costa et al. 2021). The beads considered in this work were found in nine archaeological sites in the present-day Lazio region of Italy. These sites belong to two different historic regions, commonly named Southern Etruria (Capena, Cerveteri, Falerii, Narce, Veio and Vulci) and Latium (Marino, Osteria dell'Osa and Sermoneta) in the IA archaeological scholarship. The position of the sites is reported in Figure 1, which shows a map of Italian peninsula.

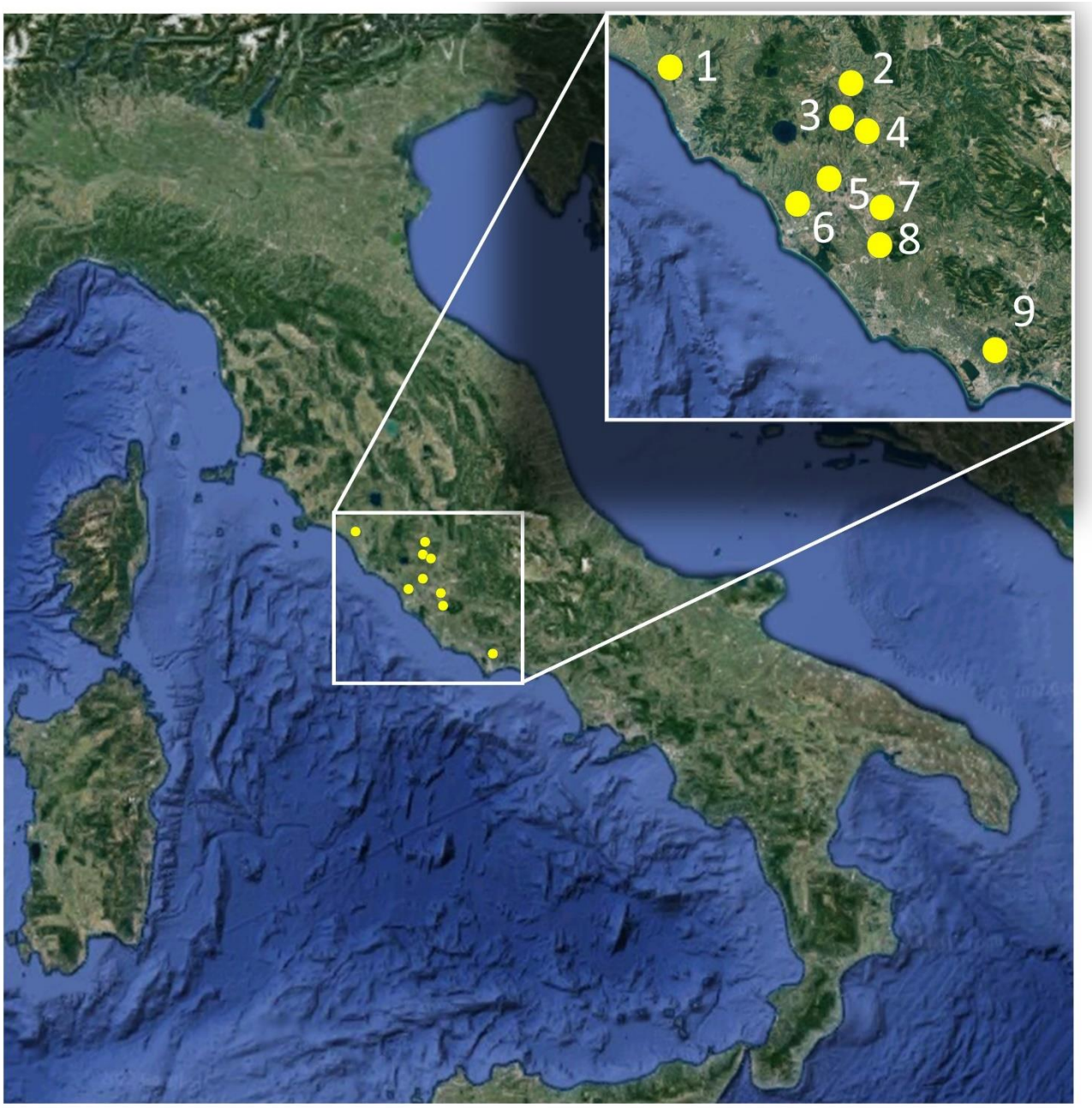

Figure 1. Location of the archaeological sites on the map of Italian peninsula. 1 – Vulci; 2 – Falerii; 3 – Narce; 4 – Capena; 5 – Veio; 6 – Cerveteri; 7 – Osteria Dell'Osa; 8 – Marino; 9 – Sermoneta.

With more details, the beads were found in twenty-one inhumations and three cremation burials (see Supplementary information, Table SI1). Many graves also contained faience and amber beads in addition to the glass ones, testifying developed trade connections, as such materials were not available locally (D'Ercole, 2017). In accordance with the burial tradition of that time, most of the graves also contained local pottery and bronze objects, although the occurrence of imported ceramics (predominantly Greek or Greek-type ware) was also frequent in this cultural milieu.

In the Mid-Tyrrhenian area, and especially in the region of Etruria, the 8th and 7th centuries BCE were times of profound social and economic changes. Settlements evolved to proto-urban and urban centres, crafts took new heights in development (Bietti Sestieri, 1997, Pacciarelli 2017) and long-distance trades resumed after the Bronze Age Collapse (Sherratt and Sherratt, 1993; Collis, 2003). This can be viewed as part of a wider 'globalising' phenomenon encompassing the entire Mediterranean area (Hodos 2020).

The deep blue colour of glass was achieved starting from the Bronze Age Egypt by the addition of cobalt to the glass batch. It was highly valued by ancient societies up to the restriction of its production and use (Barag, 2006; Hodgkinson, 2019; Schenkel, 2019). Glass makers knew several sources of cobalt. How and where these sources were exploited for the preparation of blue glass were points of debate among scholars for several decades (Sayre and Smith 1973; Henderson, 1985; Rehren, 2001; Tite and Shortland, 2003; Reade et al. 2005; Gratuze and Picon, 2005; Nikita and Henderson, 2006; Abe et al., 2012; Smirniou and Rehren 2013; Oikonomou et al. 2018; Hodgkinson et al., 2019; Costa et al., 2021 and references within). This extensive debate gives robust basis for the interpretation of compositional data for blue glass.

In this work, a non-invasive, in situ approach was adopted to highlight compositional and technological heterogeneity (if any) of ring-eye blue beads from IA Central Italy. The goal was to obtain as much information as possible directly in the museum, with a focus on technology of production (investigated through Optical Microscopy - OM), colouring agents (detected by Fibre Optics Reflectance Spectroscopy - FORS) and elemental composition (determined by portable X-Ray Fluorescence spectroscopy – p-XRF).

All the beads of this type (i. e. hundreds of specimens) preserved in the Museo Nazionale Etrusco di Villa Giulia and in the Museo delle Civiltà (both in Rome, Italy) were observed under the OM. Then, fifty-six beads were selected in order to represent this large assemblage. It is worth stressing that the investigated set of beads represents all the ring-eye blue beads found in a large set of the presently known IA archaeological sites in South Etruria and Latium, covering the entire timespan that yielded such beads. In order to integrate the results of the preliminary non-invasive screening, a selected subset of five beads was analysed in the laboratory with Scanning Electron Microscopy coupled with Energy Dispersive Spectroscopy (SEM-EDS).

2. MATERIALS AND METHODS.

2.1. Glass beads. The graves in South Etruria and Latium in which ring-eye blue beads were found belong mostly to the Early Iron Age II period (EIA II), therefore forty-five beads (i.e. the majority of the fifty-six beads considered in this work) originate from tombs of this period. Most scholars conventionally date EIA II to 800-720 BCE (see Bartoloni and Delpino 2005 for an overview on periodisation and absolute dating, with related discussions on these topics). One bead of the considered sample set dates to the Early Iron Age I (EIA I: ca 950 – 800 BCE), nine beads were found in tombs of the Orientalising period (most of them from the Early Orientalising period, which is approximately dated to 720-670 BCE). Finally, one bead is dated to the Late Archaic period (530-400 BCE).

In the selection of the samples, attention was given also to include all colour and/or translucency variations. Typical representatives of this bead type are shown in Figure 2: they are compressed spheres of 5-9 mm in diameter (dimension perpendicular to the aperture) and 3-6 mm in height (dimension along the aperture). The diameter of the aperture for the whole assemblage is 2-3 mm. All of them are semi-translucent, blue with various degrees of saturation. Most of them are decorated with 3 or, in fewer cases, 2 ring-eyes of

opaque white glass. In some of the beads, the decoration was detached and lost. Moreover, some of the beads keep integrity, while others were available as fragments.

Figure 2. Glass beads form Capena, Early Orientalising period, Museo delle Civiltà, Rome. Four beads from this set were studied with the non-invasive spectroscopic approach reported in the text. © Museo delle Civiltà, Rome.

Remains of white glass droplets instead of rings are visible on the blue-green body of sample PG112, suggesting that this bead may belong to a different type, known from the Late Bronze Age through the finds from Frattesina (Italy) (Bellintani and Angelini 2020).

2.2. Optical Microscopy (OM). A Dino-Lite AM4815ZT – Edge digital microscope was used for visual examination and documentation of the beads. All the ring-eye blue beads preserved in the two museums were observed and some images at 20× and 100× magnification were acquired. This wide set of similar beads explored under the OM highlighted some features relevant for the interpretation of the bead-forming process.

2.3. Fibre Optics Reflection Spectroscopy (FORS). An Ocean Insight HL-2000-HP-FHSA 20W Tungsten halogen light source was used to transmit light through a 2m-long reflection/backscatter fibre optics probe with 400 μm core size. The angle of the incident light beam was set around 45°, with adjustments to better capture the characteristic features of the diffuse light spectrum. Diffuse light was then transmitted to the Ocean Insight QEPro CCD detector with HC1 grating. Operating range was 248 – 1038 nm with optical resolution 6.78 nm FWHM. The instrument was calibrated using a high reflectivity Spectralon reference. The integration time was from 0.019 to 0.029 s, no less than 40 scans were averaged for a single spectrum acquisition and several spectra were acquired in different parts of each bead, including the white decorations. For these latter, the spectra did not show any characteristic band, except for those of the blue glass. Therefore, spectra of white decorations were not taken into consideration in the discussion of the data. All the spectra were normalized to 100%.

2.4. Portable X-Ray Fluorescence spectroscopy (p-XRF). Three p-XRF units were used for the analyses. One was an ELIO spectrometer (XGLab S.R.L. Milan, Italy), equipped with Rh anode source with a focusing beam spot size of 1.2 mm and a 25 mm^2 Silicon Drift Detector (SDD). A second unit was an Unisantis XMF-104 spectrometer (Geneva, Switzerland) equipped with Mo anode source, polycapillary optics focusing the beam on a spot of 80 μm and a Si-PIN detector of 7 mm^2 area. The third unit, called Frankie, was developed in house by the Italian National Institute of Nuclear Physics-LNF (INFN-LNF Frascati, Italy) and has a W anode source, polycapillary optics focusing the beam onto a spot of 300 μm and a SDD detector with an active area of 20 mm^2. Acquisition settings of these instruments were as follows (integration time, tube current, voltage):

- ELIO: 90 s; 40 μA; 40 kV.
- Unisantis: 150 s; 300 μA; 50 kV.
- Frankie: 200 s; 80 μA; 40 kV.

For each bead, both the blue glass and the white decoration were analysed in three different parts of the same bead. Nevertheless, as signals from the blue parts are likely to be included in the spectra obtained

from the white decorations due to the low thickness and small surface of these parts, elemental data for the white glass can include, at least partially, the composition of the blue glass.

Spectra were elaborated by PyMCA software (Solé et al. 2007) and elemental concentrations were calculated based on the algorithm of the Fundamental Parameters method calibrated using Corning Glass references (A, B, and D) and several archaeological glasses with known composition. The complete description of the procedures, as well as the assessment of the accuracy of the quantitative data, is given in Yatsuk et al. 2022. In this work, limits of quantification were cautiously risen for some elements after critical evaluation of the obtained spectra and are indicated in the Table 1.

2.5. Scanning Electron Microscopy coupled with Energy Dispersive Spectrometry (SEM-EDS). Five samples were analysed using this technique. Among them, three samples (namely, PG110_1, PG110_2 and PG139) were embedded in epoxy resin and prepared as polished cross sections. Two samples (namely PG156 and VG109) were analysed without any preparation at low vacuum conditions – 50 Pa (VP-SEM-EDS). The microscope was a JEOL JSM-IT300LV coupled to an EDS with SDD detector (Oxford Instruments). Operating conditions were as follows: acceleration voltage: 15 kV; acquisition time: 40 s; working distance: 10 mm. The compositional data were obtained as mean values of the compositions collected on five squares of about 10 μm^2 at 5000× magnification in the high vacuum mode and at variable magnifications in the variable pressure mode.

3. RESULTS.

3.1. OM. The visual examination through OM gave some hints on the bead-making processes. OM images (Figure 3) show that the white decorations were applied as soft threads of hot glass inlayed in the surface of the still hot blue bead, producing a thin and narrow decoration (Figure 3 top left image). In many cases, the white glass is partially or completely detached from the main body leaving a groove (Figure 3, top right). The white thread forms rounds or, more frequently, irregular ovals, and sometimes the ends of the white tread do not join (Figure 3, bottom left). The eye spot is constituted by the body of the bead itself (Figure 3, top right and bottom left), thus allowing to classify the type as simple ring-eyes beads. The blue bulk of the bead was made by winding the hot glass around a mandrel. The technique is suggested by the shape of the bead and by the slight asymmetry in the direction parallel to the aperture. Also, winding tips near one of the poles, i.e. finishing points of the glass mass that was wound around the mandrel, are visible in some specimens (Figure 3, bottom right) (Koch, 2001; Bellintani, 2011; Sprague, 1985).

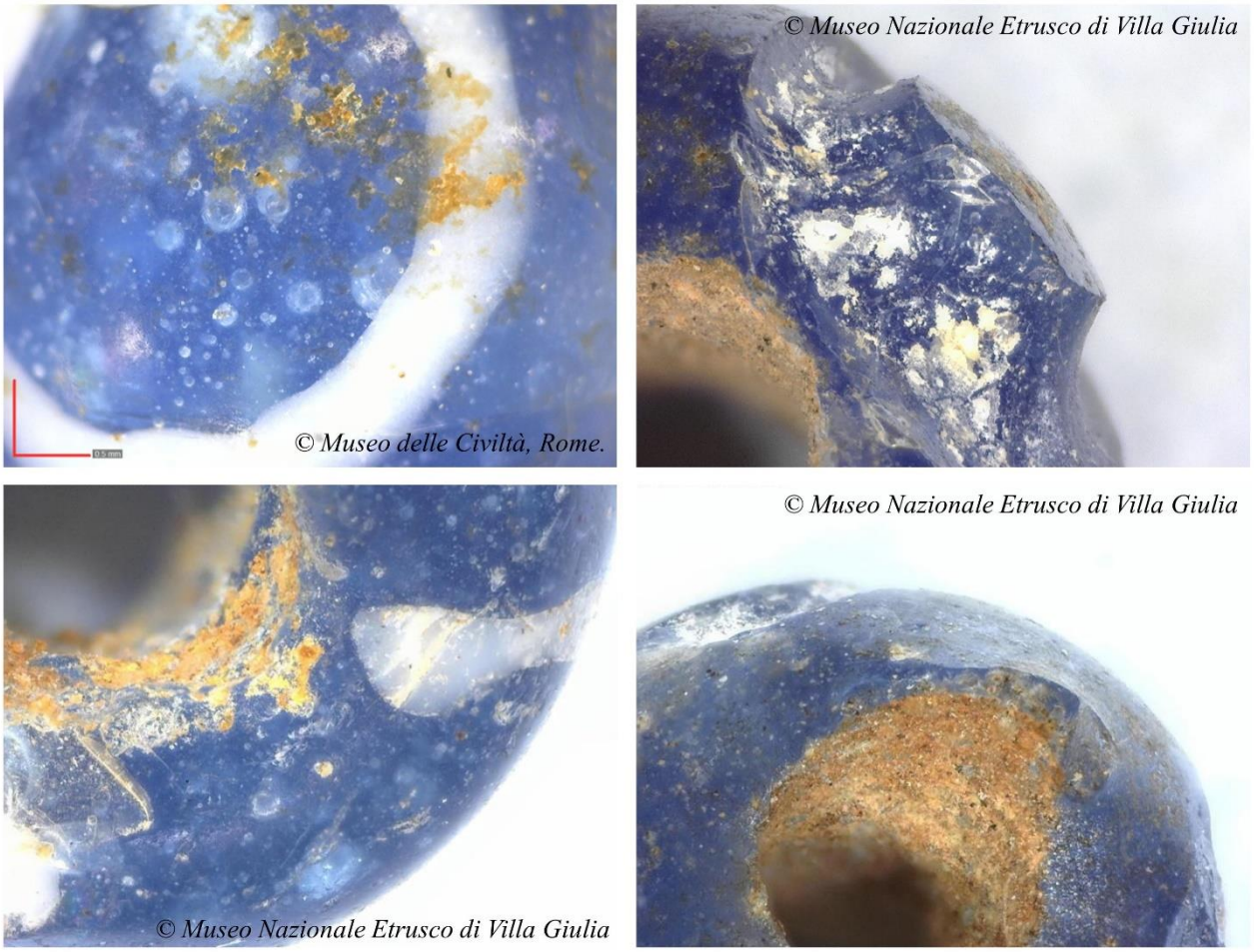

Figure 3. Microscope images of selected beads. Top left – PG44, top right – VG55, bottom left – VG35, , bottom right – VG20. The scale bar, same for all the images, is 0.5mm.

3.2. FORS. The diffuse reflectance spectra were employed to detect the colouring chemical species in the glass (values compared to ones in Micheletti et al., 2020, and references therein). The blue bulk of the beads mostly produced similar spectra, with some noticeable exceptions. Representative spectra from the whole sample set are reported in Figure 4. Most of the samples show bands similar to those reported for PG155 and VG58: in the UV-Visible region they feature the bands of Fe^{3+} at 380, 420 and 440 nm, which can be also tentatively attributed to Mn^{2+}, whereas the pronounced set of Co^{2+} triple bands at approximately 540, 600, and 640 nm, expected for soda-lime glass (Fornacelli et al. 2018), is detected in the visible region. In the NIR region, the trend of the spectra may vary within this large group of samples, due to the variable presence of Fe^{2+}, which mirrors the variability of the redox conditions in the furnace for different glass batches. Yet, reducing environment would be preferable to produce Co-blue glass (Arletti et al. 2013; Hunault et al. 2016).

For a few samples (namely PG109, 110_1, 111, 112, 138, 151, and VG72) the wide band centred at approximately 775 nm revealing Cu^{2+} is present, suggesting that this small group is Co-Cu coloured. On the other hand, PG112 does not show the Co^{2+} bands, and Cu^{2+} plays therefore the main role in producing the colour of this bead. The different colouring technique highlighted through FORS can be expected for this bead, as a different type was already suggested for this bead by the slightly different decoration.

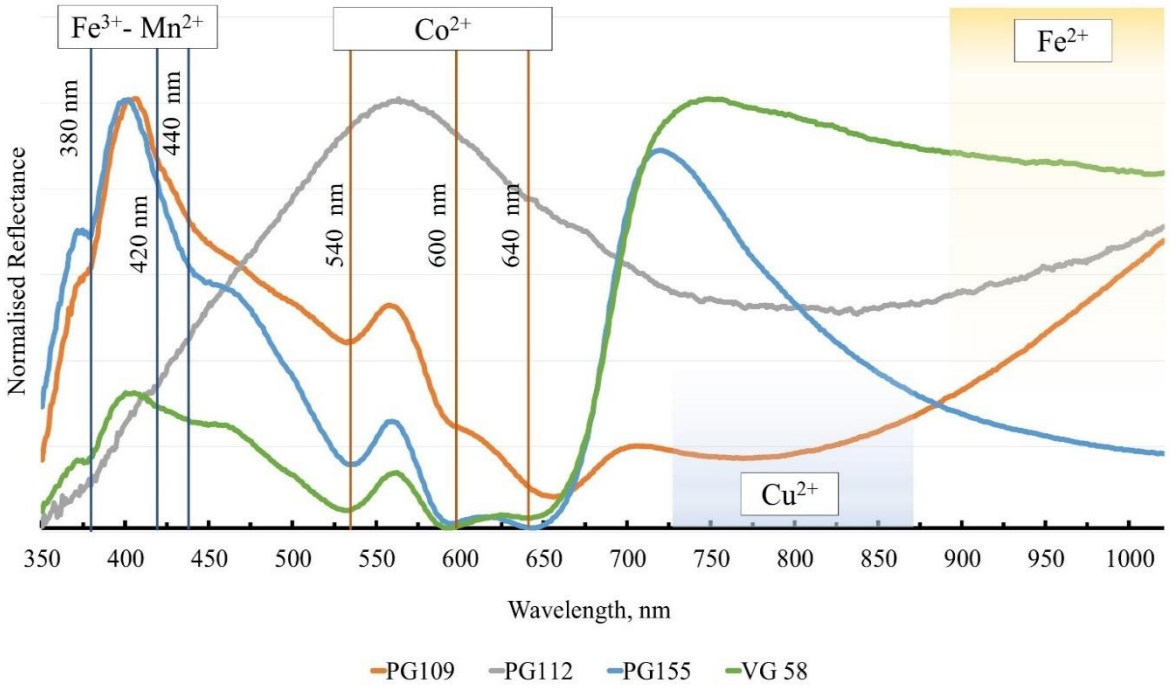

Figure 4. Representative FORS spectra for the blue part of the beads, with indicated the characteristic bands (Fe^{3+}-Mn^{2+} bands – blue vertical lines; Co^{2+} bands – brown vertical lines, Cu^{2+} - blue area, Fe^{2+} - yellow area).

3.3. p-XRF. The results of the p-XRF analyses are reported in Table 1. Concentrations for K, Ca, Ti, Mn, Fe, Co, Ni, Cu, Zn, Sr, and Sb were measured for all the samples. For some spots on a same bead, also Cr, Rb, Zr, Sn, and Pb were detected. The Limits of Quantification (LOQ) for these elements were established as follows (the highest among three instruments): Cr – 273ppm, Rb – 128ppm, Zr – 162ppm, Sn – 1417ppm, Pb – 510ppm. As the concentrations of these elements were close to the LOQs of the method, they were not considered in the discussion of the results. For the majority of the samples, K_2O concentration below 1.2% suggests the use of an evaporitic source of flux (Henderson 1985), though the use of soda-rich plant ash can be suggested for VG21 and VG113 (Rehren, 2001).

Table 1. Compositional data obtained with p-XRF (blue bases) with their respective standard deviation values. All values are represented as oxide %. Character "<" is followed by the Limit Of Quantification, which is specific for each element and p-XRF unit.

Sample name	K_2O	CaO	TiO_2	MnO	Fe_2O_3	CoO	NiO	CuO	ZnO	SrO	Sb_2O_5
PG44	<1.2	4.2	0.131	0.27	1.08	0.08	0.084	<0.4	0.047	0.032	0.16
st. dev.	-	0.6	0.002	0.02	0.02	0.02	0.007	-	0.007	0.002	0.02
PG45	<1.2	4.52	0.139	0.29	1.12	0.085	0.08	<0.4	0.053	0.033	0.18
st. dev.	-	0.09	0.009	0.03	0.01	0.006	0.02	-	0.001	0.003	0.01
PG46	<1.2	4.16	<0.12	0.31	0.68	0.079	0.063	<0.4	0.058	0.034	0.28
st. dev.	-	0.02	-	0.01	0.02	0.008	0.008	-	0.001	0.001	0.03

PG47	<1.2	5.7	0.13	0.45	0.99	0.111	0.079	<0.4	0.076	0.037	0.3
st. dev.	-	0.6	0.04	0.03	0.03	0.002	0.001	-	0.005	0.004	0.1
PG73	<1.2	3.7	0.22	0.32	1.1	0.09	0.089	<0.4	0.056	0.024	<0.087
st. dev.	-	1.7	0.01	0.09	0.3	0.03	0.008	-	0.021	0.011	-
PG77	<1.2	3.6	0.12	0.099	0.77	<0.042	0.044	<0.4	0.027	0.026	0.17
st. dev.	-	0.2	0.01	0.004	0.07	-	0.005	-	0.003	0.007	0.04
PG78	<1.2	3.6	<0.12	0.26	0.96	0.083	0.077	<0.4	0.043	0.029	<0.087
st. dev.	-	0.3	-	0.02	0.07	0.007	0.005	-	0.004	0.003	-
PG79	<1.2	4.9	<0.12	0.25	0.9	0.07	0.08	<0.4	0.049	0.033	<0.087
st. dev.	-	0.8	-	0.07	0.2	0.02	0.02	-	0.009	0.007	-
PG80	<1.2	3.7	<0.12	0.19	0.8	0.08	0.056	<0.4	0.052	0.029	<0.087
st. dev.	-	0.6	-	0.04	0.1	0.02	0.005	-	0.008	0.001	-
PG82	<1.2	4.1	<0.12	0.38	1.2	0.108	0.11	<0.4	0.056	0.033	<0.087
st. dev.	-	0.6	-	0.05	0.1	0.007	0.02	-	0.008	0.005	-
PG85	<1.2	5.9	0.144	0.25	0.9	0.068	0.07	<0.4	0.037	0.032	0.160
st. dev.	-	0.8	0.008	0.05	0.1	0.009	0.01	-	0.005	0.007	0.002
PG86	<1.2	6.1	0.18	0.39	2.2	0.11	0.11	<0.4	0.083	0.032	<0.087
st. dev.	-	0.6	0.03	0.05	0.2	0.02	0.01	-	0.006	0.001	-
PG91	<1.2	4.1	<0.12	0.22	0.7	0.07	0.07	<0.4	0.07	0.034	0.31
st. dev.	-	1.5	-	0.06	0.2	0.02	0.02	-	0.02	0.009	0.02
PG92	<1.2	4.7	0.28	0.41	1.5	0.10	0.11	0.41	0.08	0.033	<0.087
st. dev.	-	0.7	0.05	0.04	0.2	0.02	0.02	0.09	0.01	0.004	-
PG93	<1.2	4.9	0.15	0.3	0.9	0.09	0.09	<0.4	0.088	0.04	0.4
st. dev.	-	2.6	0.04	0.1	0.4	0.04	0.03	-	0.038	0.02	0.1
PG94	<1.2	4.1	0.18	0.3	1.2	0.07	0.09	0.4	0.05	0.04	0.28
st. dev.	-	1.8	0.05	0.1	0.4	0.03	0.03	0.2	0.02	0.01	0.05
PG100	<1.2	4.5	0.13	0.3	1.1	0.09	0.10	<0.4	0.12	0.03	0.24
st. dev.	-	1.3	0.04	0.1	0.5	0.04	0.04	-	0.05	0.01	0.02
PG102	<1.2	7.3	<0.12	0.18	0.72	0.07	0.05	0.45	0.051	0.028	0.6
st. dev.	-	1.0	-	0.03	0.04	0.01	0.01	0.07	0.005	0.002	0.4
PG103	<1.2	4.5	<0.12	0.26	0.8	0.07	0.08	<0.4	0.05	0.032	0.21
st. dev.	-	1.6	-	0.06	0.2	0.02	0.02	-	0.01	0.006	0.02
PG107	<1.2	1.8	0.12	0.15	0.9	<0.042	0.05	0.8	0.04	<0.010	<0.087
st. dev.	-	0.5	0.04	0.07	0.2	-	0.03	0.6	0.01	-	-
PG108	<1.2	3.3	0.18	0.20	1.2	0.06	0.05	<0.4	0.03	0.024	0.176
st. dev.	-	1.1	0.03	0.07	0.2	0.02	0.01	-	0.01	0.005	0.030
PG109	<1.2	5.1	0.12	0.59	0.44	<0.042	<0.025	0.54	<0.019	0.028	0.4
st. dev.	-	1.4	0.06	0.07	0.06	-	-	0.02	-	0.004	0.1
PG110_1	<1.2	4.7	0.14	1.1	0.5	<0.042	<0.025	0.9	<0.019	0.030	0.4
st. dev.	-	1.1	0.04	0.3	0.1	-	-	0.2	-	0.007	0.1
PG111	<1.2	4.2	<0.12	0.61	0.85	<0.042	0.06	0.53	0.038	0.026	0.73
st. dev.	-	0.3	-	0.09	0.08	-	0.01	0.06	0.007	0.003	0.05
PG112	<1.2	3.6	0.123	0.9	0.52	<0.042	<0.025	0.7	<0.019	0.028	<0.087
st. dev.	-	0.5	0.003	0.1	0.07	-	-	0.1	-	0.004	-
PG134	<1.2	2.7	0.19	0.19	0.9	0.06	0.05	<0.4	0.039	0.028	<0.087
st. dev.	-	0.8	0.06	0.06	0.3	0.02	0.01	-	0.009	0.008	-
PG138	<1.2	3.9	0.21	1.5	0.4	<0.042	<0.025	0.9	<0.019	0.04	0.3
st. dev.	-	1.3	0.06	0.6	0.1	-	-	0.4	-	0.01	0.2
PG139	<1.2	4.9	<0.12	0.3	0.5	0.09	0.08	<0.4	0.07	0.03	0.27

st. dev.	-	3.4	-	0.2	0.4	0.06	0.05	-	0.05	0.02	0.06
PG149	<1.2	3.8	0.15	0.26	0.64	0.121	0.103	<0.4	0.086	0.030	0.16
st. dev.	-	0.3	0.04	0.03	0.03	0.006	0.006	-	0.002	0.003	0.07
PG150	<1.2	4.4	0.12	0.53	1.1	0.17	0.14	<0.4	0.11	0.035	0.3
st. dev.	-	0.6	0.02	0.05	0.2	0.02	0.02	-	0.01	0.004	0.1
PG151	<1.2	4.7	0.25	0.49	1.5	0.10	0.081	<0.4	0.080	0.030	<0.087
st. dev.	-	0.3	0.02	0.06	0.1	0.01	0.007	-	0.005	0.003	-
PG152	<1.2	3.2	<0.12	0.25	0.8	0.09	0.07	<0.4	0.06	0.030	<0.087
st. dev.	-	1.1	-	0.08	0.3	0.03	0.03	-	0.02	0.007	-
PG155	1.2	3.8	0.16	0.25	1.3	0.10	0.12	<0.4	0.14	0.028	<0.087
st. dev.	0.5	0.9	0.06	0.05	0.4	0.03	0.03	-	0.04	0.007	-
PG156	<1.2	5.3	0.16	0.22	0.94	0.088	0.08	<0.4	0.076	0.035	<0.087
st. dev.	-	0.5	0.02	0.02	0.09	0.009	0.01	-	0.008	0.002	-
VG20	0.8	3.8	<0.087	0.20	0.5	0.06	0.05	0.3	0.05	0.023	<0.376
st. dev.	0.3	1.3	-	0.06	0.2	0.02	0.02	0.4	0.01	0.004	-
VG21	2.4	3.6	<0.087	0.4	1.6	0.09	0.11	0.4	0.09	0.014	<0.376
st. dev.	0.9	0.9	-	0.1	0.3	0.03	0.03	0.2	0.02	0.001	-
VG35	<0.398	3.2	<0.087	0.10	1.0	0.045	0.07	<0.015	0.08	0.015	<0.376
st. dev.	-	0.6	-	0.03	0.3	0.008	0.01	-	0.02	0.002	-
VG55	<0.398	3.4	<0.087	0.13	0.52	0.06	0.06	<0.015	0.045	0.018	<0.376
st. dev.	-	0.5	-	0.03	0.09	0.01	0.01	-	0.006	0.001	-
VG58	<0.398	3.8	<0.087	0.27	0.9	0.06	0.04	0.31	0.055	0.022	<0.376
st. dev.	-	0.3	-	0.04	0.2	0.01	0.01	0.18	0.005	0.003	-
VG60	<0.398	3.2	<0.087	0.3	1.9	0.10	0.09	0.3	0.12	0.019	<0.376
st. dev.	-	0.1	-	0.1	0.1	0.04	0.02	0.1	0.02	0.003	-
VG73	0.4	4.1	0.09	0.24	1.1	0.03	0.03	0.04	0.03	0.024	0.7
st. dev.	0.2	0.9	0.02	0.18	0.5	0.02	0.02	0.02	0.02	0.002	0.5
VG74	0.59	3.5	0.13	0.24	1.4	0.07	0.06	0.017	0.10	0.023	0.27
st. dev.	0.09	1.5	0.06	0.04	0.1	0.02	0.02	0.002	0.03	0.004	0.06
VG75	0.6	2.9	0.2	0.1	1.4	0.04	0.03	0.06	0.05	0.02	0.2
st. dev.	0.6	3.1	0.2	0.1	1.6	0.03	0.03	0.07	0.05	0.02	0.2
VG95	<0.398	4.2	<0.087	0.3	0.9	0.09	0.11	<0.015	0.09	0.022	<0.376
st. dev.	-	1.8	-	0.1	0.3	0.03	0.04	-	0.03	0.006	-
VG96	<0.398	5.5	<0.087	0.5	1.7	0.080	0.16	<0.015	0.074	0.021	<0.376
st. dev.	-	1.8	-	0.1	0.3	0.003	0.02	-	0.007	0.001	-
VG97	<0.398	3.3	<0.087	0.4	1.4	0.13	0.10	0.3	0.10	0.012	<0.376
st. dev.	-	1.1	-	0.2	0.4	0.04	0.03	0.1	0.03	0.004	-
VG100	<0.398	4.9	<0.087	0.5	1.6	0.08	0.16	<0.015	0.08	0.026	<0.376
st. dev.	-	1.5	-	0.1	0.5	0.03	0.05	-	0.02	0.005	-
VG106	0.5	4.8	0.07	0.7	0.9	0.09	0.06	0.4	0.08	0.031	0.46
st. dev.	0.1	1.1	0.02	0.2	0.2	0.02	0.01	0.2	0.02	0.002	0.02
VG107	0.48	4.5	0.10	0.30	1.1	0.04	0.04	0.09	0.036	0.022	0.28
st. dev.	0.05	0.2	0.04	0.07	0.2	0.01	0.01	0.05	0.003	0.003	0.02
VG108	0.5	4.1	0.05	0.34	0.8	0.07	0.05	0.14	0.06	0.023	0.28
st. dev.	0.1	0.9	0.01	0.08	0.2	0.02	0.01	0.01	0.01	0.001	0.03
VG109	0.6	4.3	0.2	0.3	1.2	0.05	0.04	0.07	0.08	0.026	0.2
st. dev.	0.2	1.3	0.1	0.1	0.6	0.02	0.02	0.04	0.02	0.006	0.1
VG112	0.8	2.8	0.08	0.4	1.3	0.10	0.07	0.047	0.10	<0.017	0.46
st. dev.	0.1	0.6	0.02	0.1	0.3	0.03	0.02	0.007	0.02	-	0.03

VG113	1.5	7.2	0.047	0.21	0.9	0.05	0.035	0.038	0.05	0.025	0.174
st. dev.	0.2	1.7	0.009	0.07	0.2	0.01	0.008	0.005	0.01	0.004	0.004

3.4. SEM-EDS. The results of SEM-EDS analyses for the samples mounted as cross sections (PG110_1, PG110_2 and PG139) and for those analysed without pre-treatment (PG156 and VG106) are reported in Figure 5. It presents the values of major (excluding silica) and minor oxides that reflect the content of network modifiers, stabilisers and some colourants. Their values are normalised to 100% in order to highlight the relative compositional differences among samples. Data for the samples prepared as cross sections support the hypothesis that a Na-rich flux, such as soda-rich evaporites, was used for the glass. Unfortunately, VP-SEM-EDS analyses on PG156 and VG106 highlighted sodium depletion of the surface, therefore data for these samples are not fully representative of the composition of the pristine glass.

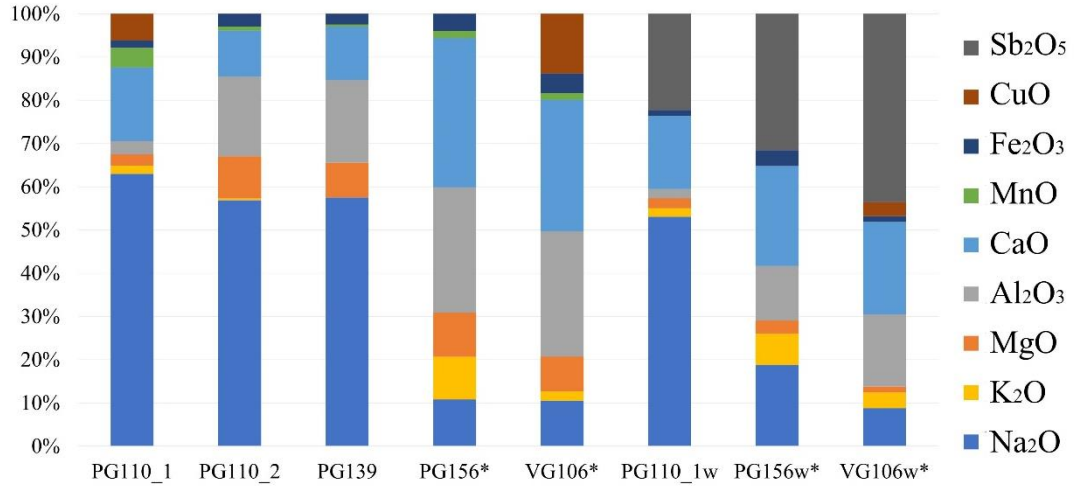

*Figure 5. SEM-EDS data for some major and minor oxides normalised to 100%. * Samples analysed without pre-treatment in variable pressure mode (data are therefore not fully representative of the composition of the pristine glass); "w" indicates white decoration.*

4. DISCUSSION.

The presence of Co, detected by FORS as Co^{2+} in tetrahedral coordination, which is responsible for the intense blue colour of the glass, was quantified by p-XRF in the range of 0.05 – 0.17 CoO %. This element was therefore added to achieve the blue colour of the beads in a range of concentration which is frequently reported in the literature for blue glass (Shortland and Tite 2000; Abe et al. 2012; Conte et al. 2016). The correlation matrix calculated for p-XRF data (Figure 6) revealed a strong positive correlation (r-values in the range from 0.71 to 0.77) within Co, Ni, and Zn, suggesting that these elements entered the batch through the same raw material. As for Fe_2O_3, the amount is consistently within the range of 0.5-1.5 %, which is enough to produce colour variations. Iron is weakly correlated with Co, Zn and Ni, therefore it is reasonable to assume that it could have entered the batch, at least partially, as an impurity of the cobalt-containing ore, although some contribution from the silica source is also expected.

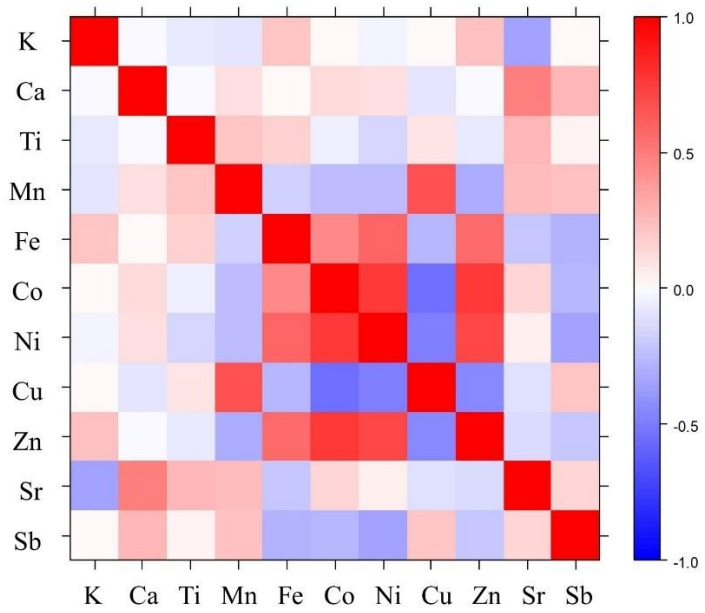

Figure 6. Correlation matrix of the data from the Table 1.

The chemical evidence linking Co, Zn and Ni can lead to further information if we compare the compositional data obtained here with those from the literature (Figure 7). Chemical composition is in fact available for blue glass from different contexts (mostly Iron Age Mediterranean), made by using cobalt ores from several sources, namely Iran, the Erzgebirge/Krušnohoří mining region, an unlocated (probably European) source and Egypt.

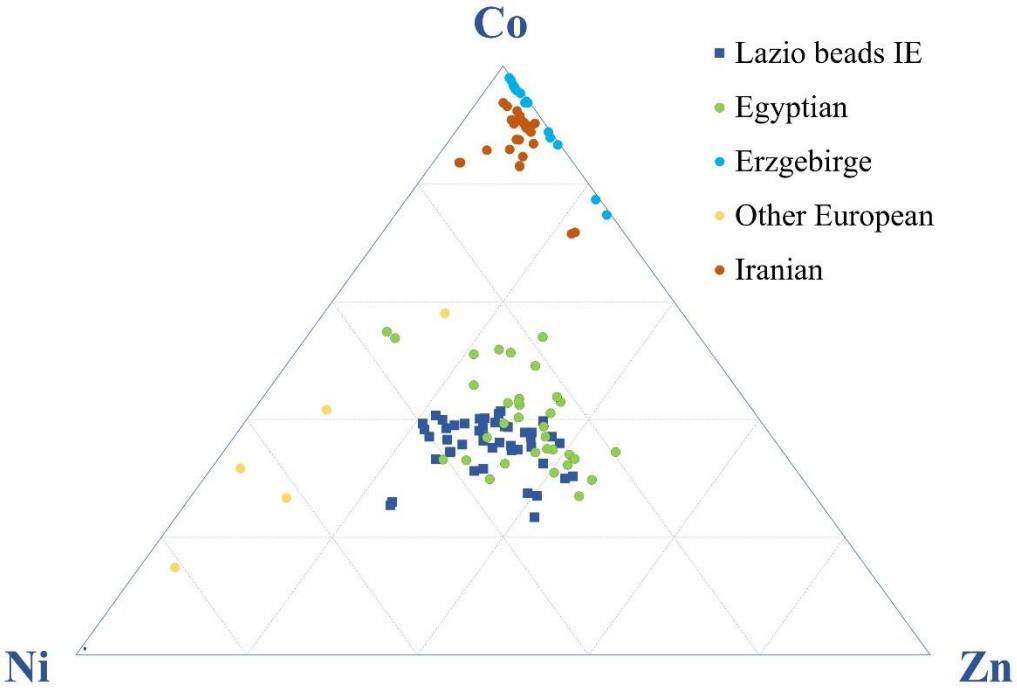

Figure 7. Ternary scatter plot of Co-Ni-Zn content in the blue parts of the beads of the present study (Lazio beads EI) and data sets of Co-coloured glasses from the literature, each representing a different source of cobalt: Egyptian from Gratuze and Picon 2005 (averaged composition), Conte et al. 2016 and Reade 2021; Erzgebirge from Costa et al. 2021; Other European sources from Towle et al. 2001 and Gratuze and Picon 2005 (averaged composition); Iranian from Oikonomou et al. 2018.

The content of Co, Zn and Ni determined in this work for the considered set of blue-eye beads resemble the composition of the blue glass coloured by using Egyptian source of cobalt, where this element was obtained from cobaltiferous alum and used since the Bronze Age (Abe, 2012). SEM-EDS data (Figure 5) also indicate that Mg and Al are abundant in the samples analysed with this technique (namely: PG110_2, PG139, PG156, and VG106). This information further substantiates the hypothesis of the use of Co-rich alum for the production process of the beads considered in the present study. The beads analysed in this work are attributed to a time-span in which the production of Co glasses in Egypt temporarily ceased (Kaczmarczyk and Hedges, 1983). Starting from the 9th century BCE, in fact, Co blue glass was produced in Nimrud (Iraq) where craftsmen apparently used evaporitic soda-rich deposits as the source of flux and Co-bearing alum as a colorant, both imported from Egypt (Reade et al., 2005).

MnO is associated with Fe_2O_3 in the majority of the samples (Figure 8, top), but it also shows another independent source for a separate group of samples. p-XRF data would suggest that the beads PG 109, 110_1, 111, 112, 138 and VG106 can be considered as a separate group of beads coloured by Co-Cu (and with substantial MnO content). This result is in good agreement with the FORS spectra.

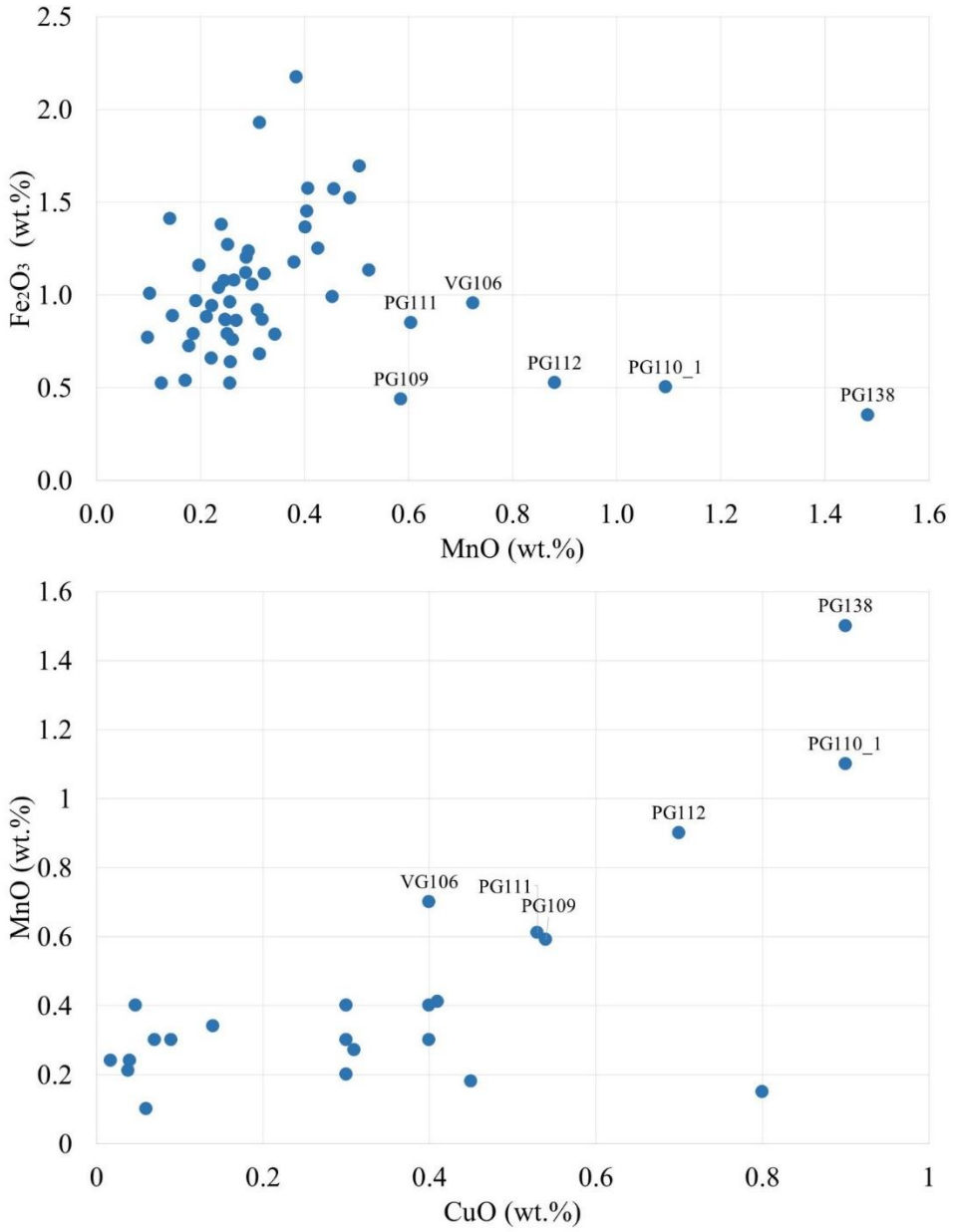

Figure 8. MnO/Fe_2O_3 (top), and CuO/MnO (bottom) binary plots of the samples analysed with p-XRF (blue bases' values only).

In these samples, Co levels were below the LOQ for p-XRF (but the samples still exhibit Co^{2+} bands when analysed with FORS). On the other hand, CuO levels of these samples are higher (0.4 – 0.9%) in comparison with the main group. Moreover, SEM-EDS data (Figure 5) for the one representative of this group analysed with the techniques, namely PG110_1, shows lower concentration of MgO and Al_2O_3 when compared with other samples of the main group analysed with the same technique. Finally, for this subset of beads, MnO concentrations show a strong positive correlation with CuO (Figure 8, bottom) which is not a commonly observed pattern. This allows us to state that the final colour of this group of samples was influenced by three, or even four elements (Mn, Fe, Co, and Cu) coming probably as separate components into the batch. This group of beads (henceforth Co-Cu coloured) encompasses beads from various archaeological periods and from different archaeological contexts, therefore, no evidence emerged based on distribution in space and time of this small heterogeneous set. The bead PG112 stands out in this picture, as Co was not detectable both with p-XRF and FORS.

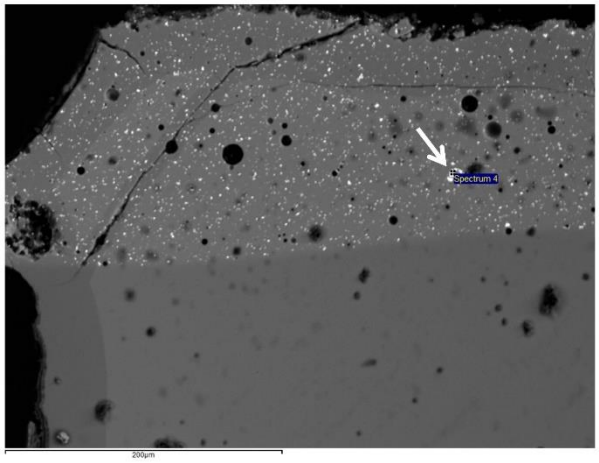

Figure 9. PG110_1 cross section BSE image; white part (top) and blue part (bottom); the point of the analysis in the white part featured some 11% of Sb_2O_5

Calcium, apparently, performs two functions in the samples. It is most of all a stabilising component of the batch, with CaO and SrO weakly positively correlated. Ratio of these oxides is higher for white parts and r value is also higher (about 0.59). The excess of Ca in white parts can be explained by the use of Ca antimonate as a colouring (and opacifying) agent, as in these parts the antimony levels detected by p-XRF are higher and the correlation coefficient between Ca and Sb is equal to 0.49. It is worth noting that Sb was frequently detected also in the blue parts of the beads, but the very small dimension of the beads does not allow us to speculate on the significance of this element in the blue body of the bead. Figure 9 demonstrates the presence of inclusions rich in Sb and Ca, that confirms the presence of calcium antimonate, a quite widespread agent for making white opaque glass (Lahlil et al. 2008).

5. CONCLUSION.

The analytical techniques combined in this study to investigate a set of white-eye blue beads selected to represent the entire *corpus* of presently known beads of this type found in South Etruria and Latium - and covering the entire timespan that yielded such beads - gave complementary information that allowed to discuss, at least preliminarily, some compositional feature of the glass batch and of the beads themselves.

OM observation of these beads indicates that they were obtained by winding hot glass around a mandrel, then the decoration was made by inlaying coils of white glass into the soft blue base.

It was established that cobalt was the major colorant, as emerged from both FORS and p-XRF data, and that calcium antimonate crystals were used to obtain the white opaque glass for the decorations, as highlighted by p-XRF and SEM-EDS data. The compositional features associate a larger part of the investigated beads with Egyptian raw materials, but the attested lack of production of Co blue glasses and faience in Egypt during the 10^{th}-7^{th} centuries BCE suggests Nimrud as the possible place of production, albeit

with Egypt still playing a role for the supply of the flux and the cobalt ore. This seems to be an initial point of a trade network that spanned the entire Mediterranean. Lands of west-Central Italy were incorporated into this network, apparently, from the 9th century BCE, but the traders (probably Phoenicians or Levantine) still need to be identified.

A smaller sub-group of beads appears to be Co-Cu coloured according to FORS, p-XRF and SEM-EDS data, demonstrating the presence of alternative tradition of glass colouring, possibly attributed to local imitation, or mirroring a change in the supply chains.

This preliminary investigation, mainly based on a non-invasive approach, gives for the first time a compositional overview on a representative set of the (apparently) homogeneous *corpus* of white-eye blue beads from IA Central Italy, suggesting a possible provenance for the majority of the beads and highlighting compositional heterogeneities that need further attention in future archaeometric investigations.

ACKNOWLEDGEMENTS. Authors express their gratitude to the administration of the Museo Nazionale Etrusco di Villa Giulia and the Museo delle Civiltà for granting permissions for the analyses. This project has received funding from the European Union's Horizon 2020 research and innovation programme under the Marie Skłodowska-Curie grant agreement No 754511. The contents of this paper are the sole responsibility of the authors and do not necessarily reflect the opinion of the European Union.

REFERENCES

Abe, Y., Harimoto, R., Kikugawa, T., Yazawa, K., Nishisaka, A., Kawai, N., Yoshimura, S., & Nakai, I. (2012). Transition in the use of cobalt-blue colorant in the New Kingdom of Egypt. *Journal of Archaeological Science*, 39(6), 1793-1808. https://doi.org/10.1016/j.jas.2012.01.021

Arletti, R., Quartieri, S., & Freestone, I. C. (2013). A XANES study of chromophores in archaeologyical glass. *Applied Physics A,111*(1), 99-108. http://dx.doi.org/10.1007/s00339-012-7341-4

Barag, D. P. (2006). Socio-economic observations on the history of ancient glass.*Annales du 17e Congrès de l'Association Internationale pour l'Histoire du Verre, Antwerp, 3-10*.

Bartoloni, G., Delpino, F., eds. (2005). Oriente e Occidente: metodi e discipline a confronto. Riflessioni sulla cronologia dell'età del Ferro italiana, *Atti Incontro di Studio (Roma 30-31 ottobre 2003), Mediterranea: Quaderni annuali dell'Istituto di studi sul Mediterraneo antico I*.

Bellintani, P. (2011). Progetto Materiali vetrosi della protostoria italiana: aggiornamenti e stato della ricerca. In *Rivista di scienze preistoriche LXI*. Firenze, Istituto italiano di preistoria e protostoria, 257-282.

Bellintani, P., Angelini, I. (2020). I vetri di Frattesina. Caratterizzazione crono-tipologica, archeometria e confronti nell'ambito della tarda età dell Bronzo dell'Europa centro-orientale e del Mediterraneo. *PADUSA Bollettino del Centro Polesano di Studi Storici, Archeologici ed Etnografici LVI*, Rovigo 71-118.

Bietti Sestieri, A. M. (1997). Italy in Europe in the Early Iron Age. *Proceedings of the Prehistoric Society*, 63, pp. 371-402. https://doi.org/10.1017/S0079497X00002498

Collis, J. (2003). The European Iron Age. London-New York, Routledge. http://dx.doi.org/10.4324/9780203442111

Conte, S., Arletti, R., Mermati, F., & Gratuze, B. (2016). Unravelling the Iron Age glass trade in southern Italy: the first trace-element analyses. *European Journal of Mineralogy*, *28(2)*, 409-433. http://dx.doi.org/10.1127/ejm/2016/0028-2516

Costa, M., Barrulas, P., Arruda, A.M. et al. (2021) An insight into the provenance of the Phoenician-Punic glass beads of the necropolis of Vinha das Caliças (Beja, Portugal). *Archaeological and Anthropological Science 13*, 149. https://doi.org/10.1007/s12520-021-01390-5

D'Ercole, M. C. (2017). 10 - Economy and trade. In Naso, A. (ed .), *Etruscology*, De Gruyter, Berlin,, 1, 143-163.

de Ferri, L., Mezzadri, F., Falcone, R., Quagliani, V., Milazzo, F., & Pojana, G. (2020). A non-destructive approach for the characterization of glass artifacts: The case of glass beads from the Iron Age Picene necropolises of Novilara and Crocefisso-Matelica (Italy). *Journal of Archaeological Science: Reports*, *29*, 102124. https://doi.org/10.1016/j.jasrep.2019.102124

Fornacelli, C., Ceglia, A., Bracci, S., & Vilarigues, M. (2018) The role of different network modifying cations on the speciation of the Co^{2+} complex in silicates and implication in the investigation of historical glasses. *Spectrochimica Acta Part A: Molecular and Biomolecular Spectroscopy*. *188*, 507-515. https://doi.org/10.1016/j.saa.2017.07.031

Gratuze, B., & Picon, M. (2005). Utilisation par l'industrie verrière des sels d'aluns des oasis égyptiennes au début du premier millénaire avant notre ère. In Borgard, P., Brun, J., & Picon, M. (Eds.), *L'alun de Méditerranée*. Publications du Centre Jean Bérard. 269-276. https://doi.org/10.4000/books.pcjb.603

Henderson, J. (1985). The raw materials of early glass production. *Oxford Journal of Archaeology*, *4*(3), 267-291. https://doi.org/10.1111/j.1468-0092.1985.tb00248.x

Hodgkinson, A. K. (2019). Manufacturing colourful glass objects in New Kingdom Egypt: a spatial and statistical analysis. In Warburton, D. and Thavapalan, S. (eds.), *Value of Colour. Material and Economic Aspects in the Ancient World*, Berlin. Edition Topoi, 125-175 https://doi.org/10.17171/3-70

Hodgkinson, A. K., Röhrs, S., Müller, K., & Reiche, I. (2019). The use of Cobalt in 18th Dynasty Blue Glass from Amarna: the results from an on-site analysis using portable XRF technology. *STAR: Science & Technology of Archaeological Research*, *5*(2), 36-52. https://doi.org/10.1080/20548923.2019.1649083

Hodos, T. (2020). The Archaeology of the Mediterranean Iron Age. A Globalising World c.1100–600 BCE, Cambridge; New York: Cambridge University Press. 336.

Hunault, M., Bauchau, F., Loisel, C., Hérold, M., Galoisy, L., Newville, M., & Calas, G. (2016). Spectroscopic investigation of the coloration and fabrication conditions of medieval blue glasses. *Journal of the American Ceramic Society*, *99*(1), 89-97.

Kaczmarczyk, A., & Hedges, R. E. (1983). Ancient Egyptian faience: an analytical survey of Egyptian faience from Predynastic to Roman times. Aris & Phillips. 548.

Koch L.C. (2011). Zur Herstellungstechnik der Perlen. In Koch L. K. *Früheisenzeitliches Glas und Glasfunde Mittelitaliens: eine Übersicht von der Villanovazeit bis zum Orientalizzante und eine Analyse der Glasperlen als Grabbeigabe des Gräberfeldes Quattro Fontanili in Veji*. Leidorf, 28-31.

Lahlil, S., Biron, I., Galoisy, L., & Morin, G. (2008). Rediscovering ancient glass technologies through the examination of opacifier crystals. *Applied Physics A,92*(1), 109-116. https://doi.org/10.1007/s00339-008-4456-8

Micheletti, F., Orsilli, J., Melada, J., Gargano, M., Ludwig, N., & Bonizzoni, L. (2020). The role of IRT in the archaeometric study of ancient glass through XRF and FORS. *Microchemical Journal*, *153*, 104388 https://doi.org/10.1016/j.microc.2019.104388

Nikita, K., & Henderson, J. (2006). Glass analyses from Mycenaean Thebes and Elateia: compositional evidence for a Mycenaean glass industry. *Journal of Glass Studies*, 71-120.

Oikonomou, A., Henderson, J., Gnade, M., Chenery, S., & Zacharias, N. (2018). An archaeometric study of Hellenistic glass vessels: evidence for multiple sources. *Archaeological and Anthropological Sciences*, *10*(1), 97-110. https://doi.org/10.1007/s12520-016-0336-x

Pacciarelli, M., (2017). The transition from village communities to protourban societies. In Naso, A. (ed.), *Etruscology*, De Gruyter, Berlin, 561-580.

Reade, W. (2021). The First Thousand Years of Glass-Making in the Ancient Near East: Compositional Analyses of Late Bronze and Iron Age Glasses. Archaeopress. 273. https://doi.org/10.2307/j.ctv1n9dk03

Reade, W., Freestone, I. C., & Simpson, S. J. (2005). Innovation or continuity? Early first millennium BCE glass in the Near East: the cobalt blue glasses from Assyrian Nimrud. *Annales du l'Association Internationale pour l'Histoire du Verre*, 16, 23-27.

Rehren, T. (2001). Aspects of the production of cobalt-blue glass in Egypt. *Archaeometry*, *43*(4), 483-489. https://doi.org/10.1111/1475-4754.00031

Sayre, E. V., & Smith, R. W. (1973). Analytical studies of ancient Egyptian glass (No. BNL-18562; CONF-730416-4). Brookhaven National Lab., Upton, NY (USA). 1-36.

Schenkel, W. (2019). Colours as viewed by the Ancient Egyptians and the explanation of this view as seen by academics studying colour. In Warburton, D. and Thavapalan, S. (eds.), *Value of Colour. Material and Economic Aspects in the Ancient World*, Berlin. Edition Topoi, 35-55. https://doi.org/10.17171/3-70

Sherratt, S., & Sherratt, A. (1993). The growth of the Mediterranean economy in the early first millennium BC. *World Archaeology*, *24*(3), 361-378. http://dx.doi.org/10.1080/00438243.1993.9980214

Shortland, A. J., & Tite, M. S. (2000). Raw materials of glass from Amarna and implications for the origins of Egyptian glass. *Archaeometry*, *42*(1), 14 1-151. http://dx.doi.org/10.1111/j.1475-4754.2000.tb00872.x

Shortland, A., Rogers, N., & Eremin, K. (2007). Trace element discriminants between Egyptian and Mesopotamian late Bronze Age glasses. *Journal of Archaeological Science*, *34*(5), 781-789. https://doi.org/10.1016/j.jas.2006.08.004

Smirniou, Melina & Rehren, Thilo. (2013). Shades of blue - cobalt-copper coloured blue glass from New Kingdom Egypt and the Mycenaean world: A matter of production or colourant source? *Journal of Archaeological Science*. *40*. 4731-4743. http://dx.doi.org/10.1016/j.jas.2013.06.029

Solé, V. A., Papillon, E., Cotte, M., Walter, P., & Susini, J. (2007). A multiplatform code for the analysis of energy-dispersive X-ray fluorescence spectra. *Spectrochimica Acta Part B: Atomic Spectroscopy*, *62*(1), 63-68. https://doi.org/10.1016/j.sab.2006.12.002

Sprague, R., & Bowers, A. W. (1985). Glass trade beads: A progress report. *Historical Archaeology*, *19*(2), 87-105. https://doi.org/10.1007/BF03373477

Tite, M. S., & Shortland, A. J. (2003). Production technology for copper-and cobalt-blue vitreous materials from the New Kingdom site of Amarna—a reappraisal. *Archaeometry*, *45*(2), 285-312. https://doi.org/10.1111/1475-4754.00109

418 Yatsuk, O., Ferretti, M., Gorghinian, A., Fiocco, G., Malagodi, M., Agostino, A. & Gulmini, M. (2022). Data from
419 multiple portable XRF units and their significance for ancient glass studies. *Molecules, 27(18)*, 6068.
420 https://doi.org/10.3390/molecules27186068